

## Low power consumption gas sensor based on In<sub>2</sub>O<sub>3</sub> nanowires in detecting hazardous gases

Nguyen Thanh Duong<sup>1\*</sup>, Nguyen Van Duy<sup>2</sup>

<sup>1</sup>Institute of Physical Technology, Academy of Military Science and Technology;

<sup>2</sup>International Training Institute for Materials Science (ITIMS), Hanoi University of Science and Technology (HUST).

\*Corresponding author: duongnth07@gmail.com

Received 14 Aug. 2023; Revised 04 Oct. 2023; Accepted 10 Nov. 2023; Published 25 Nov. 2023.

DOI: <https://doi.org/10.54939/1859-1043.j.mst.91.2023.54-62>

### ABSTRACT

Recently, gas-sensing devices have been applied popularly in a ton of distinct areas, such as environmental monitoring, breath analysis, food storage, and detectors for both indoor and outdoor hazardous gases. Many efforts have been studied the novel generation sensor that consists of the advantages, i.e. low power consumption, low-cost, and flexibility. One of the potential strategies to deal with this issue is self-heating. In this study, the self-heated In<sub>2</sub>O<sub>3</sub> nanofibers-based gas sensor was synthesized and fabricated via a chemical vapor deposition (CVD) combined with drop casting the as-prepared In<sub>2</sub>O<sub>3</sub> nanowires on the IDE electrode. The sensor indicates a high response toward H<sub>2</sub>S at the supplied power of 1200 μW (R<sub>g</sub>/R<sub>a</sub> ~ 1.35). This is attributed to the length of single In<sub>2</sub>O<sub>3</sub> nanowires (NWs), which provides a great pathway for electron transfer. The remarkable enhancement performance of the sensor is considered the first – step in the development of smart sensing devices.

**Keywords:** Self-heating; In<sub>2</sub>O<sub>3</sub> nanowire; CVD.

### 1. INTRODUCTION

In metal oxide gas sensors, the chemical reactions and physical phenomena demand thermal activation, and therefore, external heaters are an essential part of commercial gas sensors [1]. The modification of the working temperature provided by the heater makes the sensor exhibit different characteristics to target gas at various temperatures [2]. For example, Vanish Kumar et al. [3] investigated the pristine In<sub>2</sub>O<sub>3</sub> and Mg-doped In<sub>2</sub>O<sub>3</sub> in the range temperature of 150 °C ÷ 300 °C upon exposure to 10 ppm H<sub>2</sub>S. The correlation of operating temperature and selectivity of the In<sub>2</sub>O<sub>3</sub> nanocube gas sensor toward H<sub>2</sub>S and NO<sub>2</sub>, as reported in ref [4]. Namely, at room temperature, the In<sub>2</sub>O<sub>3</sub>-nanocube-based sensor exhibited good selectivity to H<sub>2</sub>S with a high response (1461 for 60 ppm H<sub>2</sub>S), meanwhile, the sensor shows excellent response toward NO<sub>2</sub> with an operating temperature of 100 °C. Many researchers revealed that the gas sensor based on metal oxide operates normally at a high temperature of 200 °C ÷ 450 °C [5]. Typically, commercial metal oxide gas sensors used in mobile or wireless networks consume a power supply of ten to hundreds of mW [6]. Due to the consumption of numerous energies generated by the heater, the flexible, long-term stability and application potential of the gas sensor is an obstacle. Therefore, the development of sensing devices that consist of advantages, i.e. low temperature, high sensitivity, and high selectivity, is crucial to enhance its application.

In the start-of-the-art sensing devices, many efficient ways are used to generate and control the level of working temperature of a sensor. For instance, the micro-electromechanical system (MEMS) technology can bring the power down to less than 30

÷ 50 mW [7] to reach temperatures up to 50 °C. However, the expensive equipment and complex fabrication process are still challenging in practical usage.

Over the last decade, self-heated gas sensors have gained interest due to the lower power consumption without an external heater and microheater [8]. The primary issue of self-heating gas sensors is applying the suitable bias voltage, which is sufficient for generating Joule heating inside the sensor, otherwise increasing its temperature [9].

Many studies revealed that the length of 1D nanomaterial (up to hundreds of microns) combined with a small diameter (approximately ten nanometres) plays a resistance pathway for electron transfer [10]. In addition, the weak thermal coupling with the Si substrate and Pt electrodes caused the Joule heat dissipation easier [11]. The sensors reach relatively high temperatures going through electrical tests even with the small amounts of electrical power dissipated during the electrical probing [12]. To date, the self-heating gas sensors based on oxide semiconductor nanowires are being deeply studied. Jin-Young Kim et al. [13] fabricated successfully pristine and Pd-functionalized CuO nanowires in detecting H<sub>2</sub>S gas. The self-heating tests showed that the Pd-functionalized gas sensor indicated the highest response to H<sub>2</sub>S in the case of low applied voltage (~ 5V). The CuO functionalized SnO<sub>2</sub>-ZnO core-shell nanowire gas sensor exhibited a higher response to H<sub>2</sub>S gas due to the self-heating effect after applying an external voltage at room temperature [14]. In Vietnam, several groups of researchers successfully prepared a self-heated gas sensor to detect hazardous gases. For instance, the self-heating networked Ag doped-SnO<sub>2</sub> nanowires sensor integrated into a portable module selectively detected H<sub>2</sub>S at low power consumption [15]. The H<sub>2</sub>S gas sensing properties are tested at different self-heating powers of 2 ÷ 10 mW. The result showed that the sensor obtained an excellent response of 21.2 to 0.5 ppm H<sub>2</sub>S at a low heating power of 2 mW, and it is damaged in the case of increasing heating power of over 20 mW. Up to now, there are a few publications related to In<sub>2</sub>O<sub>3</sub> nanowire-based self-heating gas sensors. Here, we focus on the development of a self-heated gas sensor based on In<sub>2</sub>O<sub>3</sub> nanowires by the combination of chemical vapor deposition on the gold substrate and drop-coating the In<sub>2</sub>O<sub>3</sub> nanowires on the sensing surface of the sensor.

## 2. EXPERIMENTAL SECTION

### 2.1. Synthesis of In<sub>2</sub>O<sub>3</sub> nanowire by the chemical vapor deposition method

In this work, In<sub>2</sub>O<sub>3</sub> nanowires have been synthesized by the CVD method, namely In<sub>2</sub>O<sub>3</sub> nanowires are grown on Si substrate pre-deposited thin film of Au. Chemicals agents used in the process include commercial powder, isopropanol solvent. All chemicals are analytical chemicals with a high purity of 99.9%. The Al<sub>2</sub>O<sub>3</sub> ceramic boat containing approximately 0.1 g Indium powders was placed in the center of a quartz tube, as shown in figure 1. The 1x1 cm Gold coated Si substrate was also placed in the middle of the Al<sub>2</sub>O<sub>3</sub> ceramic boat in a horizontal furnace.

At first, the entire CVD system was introduced with the high purity N<sub>2</sub> with a flow rate of 300 sccm for 5 min to purge the air in the quartz tube. To transport the indium vapor, the furnace was quickly heated up to 810 °C for 15 minutes with a heating rate of 36 °C.min<sup>-1</sup> and kept at that temperature for 20 minutes. Increasing temperature aims to sufficient thermal for the evaporation of Indium material. The CVD process was carried

out at a temperature of 810°C, and the vacuum pressure was down to 10-2 Torr, oxygen gas flow of 0.5 sccm was introduced into the tube in 20 min to occur the chemical reaction and form  $\text{In}_2\text{O}_3$  nanowires. Gray-white layers were observed on the Si substrate after finishing the CVD system. To enhance crystallite properties after the growing process, this Si substrate is annealed at 350 °C within 3 hours. After thermal treatment, the substrate is placed in a sample-containing tube, which includes 20 ml of isopropanol solvent and sonicated in the bath for 30 s. The obtained  $\text{In}_2\text{O}_3$  solution is used in the sensor fabrication.

The morphologies and microstructure of the  $\text{In}_2\text{O}_3$  NWs were observed by field emission scanning electron microscopy (FESEM) and X-ray powder diffraction spectra with Cu  $K\alpha$  radiation ( $\lambda = 1.54056 \text{ \AA}$ ). The  $2\theta$  range was from  $10^\circ$  to  $70^\circ$  with a scan step of  $0.02^\circ$ .

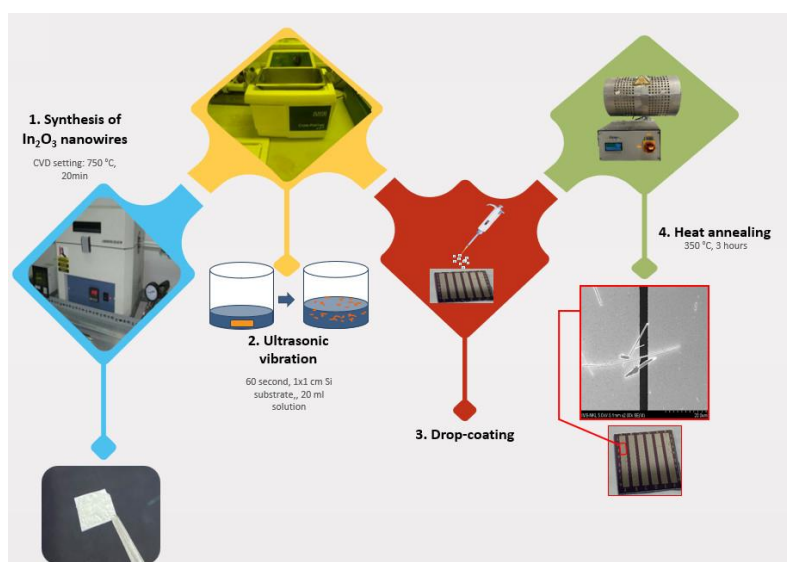


*Figure 1. CVD system used for the growth and fabrication of self-heating  $\text{In}_2\text{O}_3$  nanowires gas sensor.*

## 2.2. Fabrication of self-heating $\text{In}_2\text{O}_3$ gas sensor

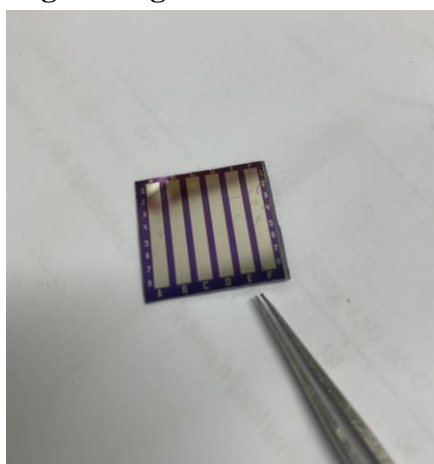


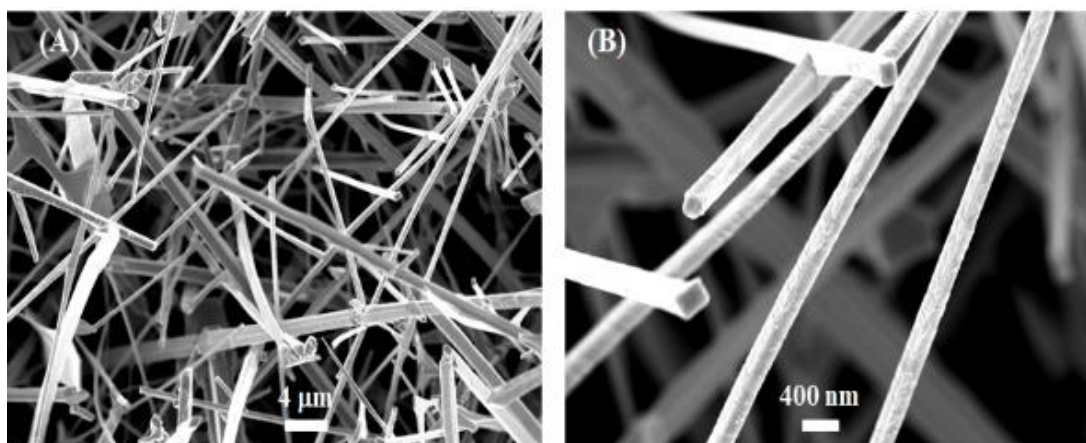
*Figure 2. Sensor after drop-coating  $\text{In}_2\text{O}_3$  NWs solution and annealing.*

The  $\text{In}_2\text{O}_3$  nanowires solution was then drop-casting on the Pt electrode surface, afterward, it was a soft break on the heating plate and thermal treatment at  $350\text{ }^\circ\text{C}$  for 3 hours to reach stability. The sensor characteristic is investigated at the different applied voltages at room temperature ( $\sim 25\text{ }^\circ\text{C}$ ) without the need for an external heater. Details about gas measurement are reported elsewhere [10]. The response is carried out by introducing the gas into the chamber in several hundred seconds by mixing the target gas and dry air (total flow rate of 400 sccm), whereas it is filled by the dry air to refresh the chamber. The sensor response is determined by the ratio of transient resistance in the case of the presence or removal of the target gases ( $S = R_g/R_a$ ). We also calculated the power consumption of the sensor using the following formula:  $P = U^2/R$ , where  $U$  is the bias voltage and  $R$  is the sensor resistance at the measured point.

### 3. RESULTS AND DISCUSSION

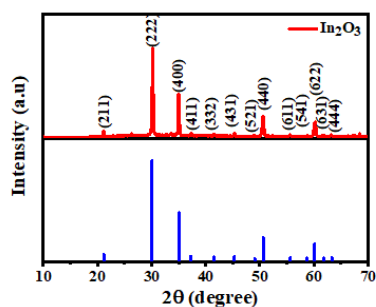
#### 3.1. Morphology and crystallinity analysis of the as-prepared $\text{In}_2\text{O}_3$ nanowires

Figure 3(A) shows the low magnification FE-SEM micrograph of as-prepared  $\text{In}_2\text{O}_3$  NWs on the Au substrate. It is observed that the pristine  $\text{In}_2\text{O}_3$  NWs has branch structure with different diameter. In addition, the nanowires are grown randomly orientation without contamination. The diameter of  $\text{In}_2\text{O}_3$  NWs was determined at about 200 nm in figure 1(B). The length of  $\text{In}_2\text{O}_3$  NWs is attributed to the Joule effect, which generates thermal for enhancement of gas response.



**Figure 3.** FE-SEM image of  $\text{In}_2\text{O}_3$  nanowires grown on the Au substrate at (A) low magnification and (B) high magnification.

To confirm the substance composition and crystallinity structure of the as-synthesized  $\text{In}_2\text{O}_3$  NWs, XRD characterization was examined. As shown in figure 3, the measured diffraction peaks matched well with the standard spectrum of the cubic phase of  $\text{In}_2\text{O}_3$  (JCPDS No. 71–2194) with a lattice constant of  $10.12\text{ \AA}$  [16]. The diffraction peaks characterized at  $2\theta$  of  $21.14^\circ$ ,  $30.08^\circ$ ,  $35.02^\circ$ ,  $37.21^\circ$ ,  $41.54^\circ$ ,  $45.25^\circ$ ,  $49.06^\circ$ ,  $50.60^\circ$ ,  $55.62^\circ$ ,  $58.77^\circ$ ,  $60.08^\circ$ ,  $61.73^\circ$ , and  $63.28^\circ$ , corresponding to (211), (222), (400), (411), (332), (431), (521), (440), (611), (622), (633) crystalline planes, respectively [17]. The sharp and high-intensity peaks demonstrated good crystallization. It can be seen that there are no impurities from other peaks. The particle size of  $\text{In}_2\text{O}_3$  was determined at about 42.6 nm from the diffraction peak via the Debye Scherrer formula [18].



**Figure 4.** XRD pattern of the  $\text{In}_2\text{O}_3$  nanowires after annealing at  $350^\circ\text{C}$  for 2h in airflow.

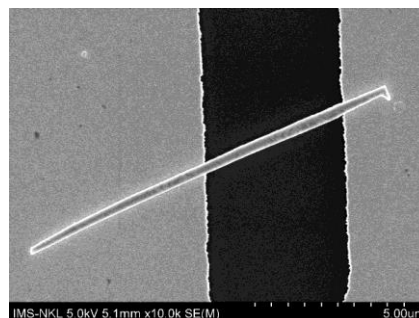
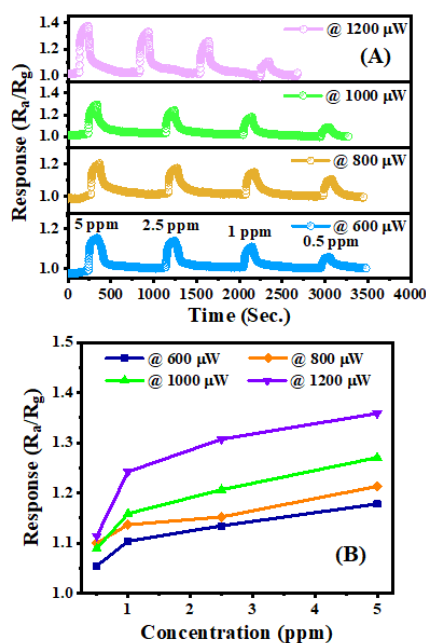


**Figure 5.** FE-SEM image of  $\text{In}_2\text{O}_3$  nanowires on Pt electrode surface.

From the above analysis, the  $\text{In}_2\text{O}_3$  NWs have successfully synthesized and have promising properties in the  $\text{H}_2\text{S}$  gas sensor.

### 3.2. Gas sensing properties of $\text{In}_2\text{O}_3$ NWs

The gas-sensing properties of the as-prepared sensor were studied at different  $\text{H}_2\text{S}$  concentrations in the self-heating mode at a room temperature of  $25^\circ\text{C}$ . The heating power was determined by the formula:  $P = U^2/R$ , where  $U$  is the applied voltage of the sensor, and  $R$  is the based resistance of the sensor. To understand the gas sensing properties, the heating power is increased by changing voltage, however, these sensors can be damaged in the case of the applied voltage up to a critical value. In our work, the sensor is tested with a maximum power of  $1200 \mu\text{W}$  (maximum applied voltage of less than 3 V).



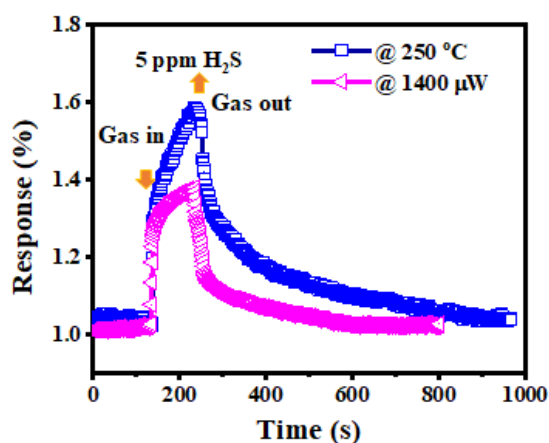
**Figure 6.** The transient response of self-heated  $\text{In}_2\text{O}_3$  gas sensor versus time at different power of 600, 800, 1200, 1400  $\mu\text{W}$  (A) and the function of response with concentration  $\text{H}_2\text{S}$  gas (B).

Figure 6(A) shows the transient response characteristics of the  $\text{In}_2\text{O}_3$  sensor when testing with  $\text{H}_2\text{S}$  gas with four applied powers. The dynamic response tends to decrease after exposure to various concentrations in the range of 0.5, 1, 2.5, and 5 ppm. This demonstrated the nature of the n-type semiconductor of  $\text{In}_2\text{O}_3$  nanowires. Namely, when the sensor is exposed to reducing gas (i.e.  $\text{H}_2\text{S}$ ), the gas molecules adsorb on the surface of nanowires and occur in a chemical reaction, leading to an increase in the electron density of the conduction band. Otherwise, the resistance of the sensor tends to decrease. The response of the sensor increased with an increase in supplied power in the measured range of  $600 \div 1400 \mu\text{W}$ . The maximum response of the sensor to 5 ppm  $\text{H}_2\text{S}$  gas at  $1400 \mu\text{W}$  was about 1.35, and the response decreased with a decrease in concentration gases ( $R_a/R_g \sim 1.1$  at  $600 \mu\text{W}$ ). The variation of gas response of the sensor at different power heating is attributed to the self-heating effect. The higher the temperature generated by an applied voltage, the easier thermal excitation, as shown in figure 6(B).

As table 1 shows, we have significantly reduced the operating voltage of the sensor to about just 5V, the concentration of testing  $\text{H}_2\text{S}$  gas greatly decreased. However, the response still stays about the same as previous studies ITIMS with the same approach method.

**Table 1.** Comparison with previous study at ITIMS with the same approach method.

Material	Method	Heating power ( $\mu\text{W}$ )	Response	Operating voltage (V)	Ref
$\text{SnO}_2$	CVD	90	1.4 (200 ppm $\text{H}_2\text{S}$ )	40	[19]
$\text{In}_2\text{O}_3$	CVD	1060	1.2 (1000 ppm $\text{H}_2\text{S}$ )	1.5	[20]
$\text{In}_2\text{O}_3$	CVD/Drop casting	1200	1.2 (5 ppm $\text{H}_2\text{S}$ )	5	This study



**Figure 7.** Response characteristic of  $\text{In}_2\text{O}_3$  – nanowires gas sensor toward 5 ppm  $\text{H}_2\text{S}$  at  $250 \text{ }^\circ\text{C}$  and self-heating with a power consumption of  $1400 \mu\text{W}$ .

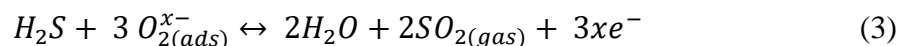
Compared to the external thermal, the self-heating  $\text{In}_2\text{O}_3$  sensor with an applied power of  $1400 \mu\text{W}$  exhibited a high-speed response to 5 ppm  $\text{H}_2\text{S}$  with the response and recovery

time of 43 s and 236 s, whereas its value reaches about 242 s and 437 s in term of 250 °C. Anyhow, the In<sub>2</sub>O<sub>3</sub> sensor showed a lower response in the case of operating at room temperature (figure 6). This is caused by the number of generated oxygen species on the surface of the In<sub>2</sub>O<sub>3</sub> nanowires at room temperature being smaller than that of 250 °C.

The sensing mechanism of the self-heated In<sub>2</sub>O<sub>3</sub> gas sensor is adsorption/desorption on the surface of nanowires. The heating region provided thermal energy, which is sufficient to activate the oxygen species (O<sub>2</sub><sup>-</sup>, O<sup>-</sup>, O<sup>2-</sup>), resulting in band bending and forming the depletion region.



The chemisorbed oxygen species act as acceptors and capture electrons, and there is an increase in the resistance of In<sub>2</sub>O<sub>3</sub> nanowires. When the In<sub>2</sub>O<sub>3</sub> nanowires were exposed to H<sub>2</sub>S gas, the target molecules reacted with the previously adsorbed oxygen into SO<sub>2</sub> and H<sub>2</sub>O, as following equations [21].



The captured electron will be released back to the conduction band. Hence, there is a decrease in the resistance of the In<sub>2</sub>O<sub>3</sub> nanowires. The resistance of the sensor turns to initial baseline resistance after introducing fresh air.

#### 4. CONCLUSIONS

In this work, we focus on the fabrication and testing of the H<sub>2</sub>S gas characteristic of the self-heated In<sub>2</sub>O<sub>3</sub> nanowires sensor via a one-step CVD technique and drop-casting on the IDE electrode. The obtained In<sub>2</sub>O<sub>3</sub> nanowires were distributed randomly with a diameter of approximately 200 nm. The XRD pattern shows that the crystalline structure of In<sub>2</sub>O<sub>3</sub> indicates a cube phase without impurity of the peak. The self-heated In<sub>2</sub>O<sub>3</sub> gas sensor was measured at room temperature (~25 °C) with different applied power toward H<sub>2</sub>S gas. The sensor response was 1.33 to 500 ppm H<sub>2</sub>S at an optimal power of 1200 μW, which is sufficient to activate the reaction for the detection of reducing gas. This performance was better than the state-of-the-art microheater gas sensor. The sensor is a potential candidate for applications related to H<sub>2</sub>S detection, such as breath exhaled analysis and environmental monitoring.

#### REFERENCES

- [1]. L. Xiao, S. Xu, G. Yu, and S. Liu, "Efficient hierarchical mixed Pd/SnO<sub>2</sub> porous architecture deposited microheater for low power ethanol gas sensor," *Sensors Actuators B Chem.*, vol. 255, pp. 2002–2010, (2018), doi: 10.1016/j.snb.2017.08.216.
- [2]. Y.-J. Hsiao, Z.-H. Shi, Y. Nagarjuna, Z.-Y. Huang, T.-Y. Lai, and S. Wu, "Double-Layered NiO/SnO<sub>2</sub> Sensor for Improved SO<sub>2</sub> Gas Sensing with MEMS Microheater Device," *ECS J. Solid State Sci. Technol.*, vol. 11, no. 5, p. 057002, (2022), doi: 10.1149/2162-8777/ac71c7.
- [3]. V. Kumar, S. M. Majhi, K.-H. Kim, H. W. Kim, and E. E. Kwon, "Advances in In<sub>2</sub>O<sub>3</sub>-based materials for the development of hydrogen sulfide sensors," *Chem. Eng. J.*, vol. 404, p. 126472, (2021), doi: 10.1016/j.cej.2020.126472.

- [4]. Z. Li et al., “Significantly enhanced temperature-dependent selectivity for NO<sub>2</sub> and H<sub>2</sub>S detection based on In<sub>2</sub>O<sub>3</sub> nano-cubes prepared by CTAB assisted solvothermal process,” *J. Alloys Compd.*, vol. 816, p. 152518, (2020), doi: 10.1016/j.jallcom.2019.152518.
- [5]. C. Zhang, Y. Luo, J. Xu, and M. Debliquy, “Room temperature conductive type metal oxide semiconductor gas sensors for NO<sub>2</sub> detection,” *Sensors Actuators A Phys.*, vol. 289, pp. 118–133, (2019), doi: 10.1016/j.sna.2019.02.027.
- [6]. F. Rasch et al., “Highly selective and ultra-low power consumption metal oxide based hydrogen gas sensor employing graphene oxide as molecular sieve,” *Sensors Actuators B Chem.*, vol. 320, p. 128363, (2020), doi: 10.1016/j.snb.2020.128363.
- [7]. J.-H. Kim, A. Mirzaei, H. W. Kim, and S. S. Kim, “Pd-functionalized core-shell composite nanowires for self-heating, sensitive, and benzene-selective gas sensors,” *Sensors Actuators A Phys.*, vol. 308, p. 112011, (2020), doi: 10.1016/j.sna.2020.112011.
- [8]. J. Seo, Y. Lim, and H. Shin, “Self-heating hydrogen gas sensor based on an array of single suspended carbon nanowires functionalized with palladium nanoparticles,” *Sensors Actuators B Chem.*, vol. 247, pp. 564–572, (2017), doi: 10.1016/j.snb.2017.03.038.
- [9]. S. M. Majhi, A. Mirzaei, H. W. Kim, S. S. Kim, and T. W. Kim, “Recent advances in energy-saving chemiresistive gas sensors: A review,” *Nano Energy*, vol. 79, p. 105369, (2021), doi: 10.1016/j.nanoen.2020.105369.
- [10]. H. M. Tan et al., “Novel Self-Heated Gas Sensors Using on-Chip Networked Nanowires with Ultralow Power Consumption,” *ACS Appl. Mater. Interfaces*, vol. 9, no. 7, pp. 6153–6162, (2017), doi: 10.1021/acsami.6b14516.
- [11]. E. Strelcov, S. Dmitriev, B. Button, J. Cothren, V. Sysoev, and A. Kolmakov, “Evidence of the self-heating effect on surface reactivity and gas sensing of metal oxide nanowire chemiresistors,” *Nanotechnology*, vol. 19, no. 35, p. 355502, (2008), doi: 10.1088/0957-4484/19/35/355502.
- [12]. C. Fàbrega, O. Casals, F. Hernández-Ramírez, and J. D. Prades, “A review on efficient self-heating in nanowire sensors: Prospects for very-low power devices,” *Sensors Actuators B Chem.*, vol. 256, pp. 797–811, (2018), doi: 10.1016/j.snb.2017.10.003.
- [13]. J.-Y. Kim, J.-H. Lee, J.-H. Kim, A. Mirzaei, H. Woo Kim, and S. S. Kim, “Realization of H<sub>2</sub>S sensing by Pd-functionalized networked CuO nanowires in self-heating mode,” *Sensors Actuators B Chem.*, vol. 299, p. 126965, (2019), doi: 10.1016/j.snb.2019.126965.
- [14]. J.-H. Kim, A. Mirzaei, J. H. Bang, H. W. Kim, and S. S. Kim, “Selective H<sub>2</sub>S sensing without external heat by a synergy effect in self-heated CuO-functionalized SnO<sub>2</sub>-ZnO core-shell nanowires,” *Sensors Actuators B Chem.*, vol. 300, p. 126981, (2019), doi: 10.1016/j.snb.2019.126981.
- [15]. T. M. Ngoc et al., “Self-heated Ag-decorated SnO<sub>2</sub> nanowires with low power consumption used as a predictive virtual multisensor for H<sub>2</sub>S-selective sensing,” *Anal. Chim. Acta*, vol. 1069, pp. 108–116, (2019), doi: 10.1016/j.aca.2019.04.020.
- [16]. B. Zhang et al., “High-performance room temperature NO<sub>2</sub> gas sensor based on visible light irradiated In<sub>2</sub>O<sub>3</sub> nanowires,” *J. Alloys Compd.*, vol. 867, p. 159076, (2021), doi: 10.1016/j.jallcom.2021.159076.
- [17]. Y. Che, G. Feng, T. Sun, J. Xiao, W. Guo, and C. Song, “Excellent gas-sensitive properties towards acetone of In<sub>2</sub>O<sub>3</sub> nanowires prepared by electrospinning,” *Colloid Interface Sci. Commun.*, vol. 45, p. 100508, (2021), doi: 10.1016/j.colcom.2021.100508.
- [18]. A. O. Bokuniaeva and A. S. Vorokh, “Estimation of particle size using the Debye equation and the Scherrer formula for polyphasic TiO<sub>2</sub> powder,” *J. Phys. Conf. Ser.*, vol. 1410, no. 1, p. 012057, (2019), doi: 10.1088/1742-6596/1410/1/012057.

- [19]. N. D. Chinh, N. Van Toan, V. Van Quang, N. Van Duy, N. D. Hoa, and N. Van Hieu, "Comparative  $NO_2$  gas-sensing performance of the self-heated individual, multiple and networked  $SnO_2$  nanowire sensors fabricated by a simple process," *Sensors Actuators B Chem.*, vol. 201, pp. 7–12, (2014), doi: 10.1016/j.snb.2014.04.095.
- [20]. D. N. Son et al., "A novel design and fabrication of self-heated  $In_2O_3$  nanowire gas sensor on glass for ethanol detection," *Sensors Actuators A Phys.*, vol. 345, p. 113769, (2022), doi: 10.1016/j.sna.2022.113769.
- [21]. Y. Wang et al., "Room temperature  $H_2S$  gas sensing properties of  $In_2O_3$  micro/nanostructured porous thin film and hydrolyzation-induced enhanced sensing mechanism," *Sensors Actuators B Chem.*, vol. 228, pp. 74–84, (2016), doi: 10.1016/j.snb.2016.01.002.

## TÓM TẮT

### Cảm biến khí dây nano Indi Oxit tiêu thụ năng lượng thấp ứng dụng trong phát hiện khí độc

Gần đây, các thiết bị cảm biến khí đang được sử dụng rộng rãi trong rất nhiều lĩnh vực như theo dõi chất lượng môi trường, phân tích hơi thở, lưu trữ thực phẩm hay phát hiện khí độc trong nhà và ngoại môi trường. Các nghiên cứu đã nỗ lực để tạo ra cảm biến thế hệ mới với ưu điểm là tiêu thụ điện năng thấp, chi phí thấp, linh hoạt. Một trong những cách tiếp cận tiềm năng để giải quyết vấn đề này là dựa trên nguyên lý tự đốt nóng của vật liệu. Trong nghiên cứu này, cảm biến khí dựa trên sợi nano  $In_2O_3$  tự gia nhiệt được tổng hợp và chế tạo thông qua quá trình lắng đọng hơi hóa học (CVD) kết hợp với phương pháp nhỏ phủ các dây nano  $In_2O_3$  đã chuẩn bị trên điện cực IDE. Cảm biến cho thấy phản hồi cao đối với  $H_2S$  ở mức công suất được cung cấp là  $1200 \mu W$  ( $R_g/R_a \sim 1,35$ ). Điều này là do chiều dài của các dây nano  $In_2O_3$  đơn lẻ (NW) tạo ra một kênh dẫn tuyệt vời cho quá trình truyền điện tử. Hiệu suất nâng cao vượt trội của cảm biến được coi là bước đầu tiên trong quá trình phát triển các thiết bị cảm biến thông minh.

**Từ khóa:** Tự đốt nóng; Dây nano  $In_2O_3$ ; CVD.